J Geophys (1987) 62:38–49

Journal of Geophysics

Seismic response of two-dimensional absorbing structures by the ray method

P. Moczo [1], P.-Y. Bard [2], and I. Pšenčík [3]

[1] Geophysical Institute, Centre of Geoscience Research, Slovak Academy of Sciences, Dúbravská cesta, 84228 Bratislava, Czechoslovakia
[2] Université Scientifique et Médicale de Grenoble, Laboratoire de Géophysique Interne et Tectonophysique, I.R.I.G.M., BP 68, F-38402 St. Martin d'Héres, Cedex, France
[3] Geophysical Institute, Czechoslovak Academy of Sciences, Boční II, 14131 Praha 4, Czechoslovakia

Abstract. A method of seismic response analysis of $2-D$ inhomogeneous structures, based on the ray method and on the application of the Debye procedure to include slight absorption, is presented. Program package RESPO, designed for such an analysis of the seismic response on the free surface of a general $2-D$ laterally varying, geological near-surface structure assuming *P*, *SV* or *SH* plane-wave incidence from below, is briefly described. The package is tested on the classical model of a sedimentary basin. The study differs from previous applications of the ray method to the basin model in the following aspects. The frequency-domain approach is used. A comparison of the ray method results with the results of the discrete wavenumber method for long periods is made. More attention is paid to the analysis of the formation of the wave field. This analysis reveals two main types of wave propagation inside the basin: the dominant horizontally propagating local interference waves and less expressive vertically propagating waves in the central part of the basin. Effects of slight absorption (Futterman's causal absorption) are considered. The absorption causes a decrease in amplitudes and time delays at later times. The decrease in the amplitudes is not so expressive because of large periods and relatively short travel times of the waves investigated.

Key words: Seismic response – Ray method – Frequency-domain approach – Slight causal absorption – Classical basin problem

Introduction

Surface and subsurface topography and/or the presence of sediments on a rock basement can cause local anomalies of ground motion or of a macroseismic field. These local effects have been studied by observing macroseismic effects, instrumentally and also theoretically. The instrumental and theoretical (e.g., numerical) methods enable the transfer properties of local geological structures to be studied. An advantage of the instrumental methods is that they simplify neither the local structure nor the incident wave field. The principal advantage of the numerical methods is that they enable us to predict a time history of vibrations and make possible detailed parametric studies and a physical understanding of the wave phenomena. A detailed insight into the wave field in the local structures has not only a theoretical meaning. The understanding of the basic wave phenomena allows us to make the first qualitative judgement of the seismic mobility of a site assuming certain knowledge of the geological structure; this helps, e.g., in better organization of experiments at the site. Finally, understanding the basic wave phenomena obtained for a certain group of exciting signals enables us to generalize conclusions on the seismic mobility of a site due to other exciting signals.

Various methods have been used to compute the seismic response of local geological structures. Let us mention the matrix method (Johnson and Silva, 1981), the finite-difference method (Zahradník and Hron, 1986), the discrete wavenumber method (Bard and Gariel, 1986), the boundary integral method (Dravinski, 1983; Sanchez-Sesma et al., 1985) and analytical methods (Yerokhin, 1985). The ray method has been used by Hong and Helmberger (1978), Langston and Lee (1983), Lee and Langston (1983a, b) and Moczo et al. (1986). The Gaussian beam method has also been used for this purpose by Nowack and Aki (1984). Only some recent papers have been mentioned here, in which a number of other references can be found.

Hong and Helmberger (1978), Langston and Lee (1983) and Lee and Langston (1983a, b) successfully used simple variants of the ray method to study seismic responses of simple models of sedimentary basins. Their success and the availability of program package SEIS83 (Červený and Pšenčík, 1984) that makes ray computations possible in more general $2-D$ laterally varying, possibly absorbing media have led us to a modification of SEIS83 to program package RESPO (Moczo et al., 1985). RESPO is designed for the computation of the seismic response on the free surface of $2-D$ laterally inhomogeneous geological near-surface structures, assuming incidence of a *P*, *SV* or *SH* plane wave from below. To test RESPO, the classical model of the sedimentary basin (Boore et al., 1971) was used. The presented study differs from the study of Hong and Helmberger (1978) and Lee and Langston (1983a) in several aspects. The frequency-domain approach is used here. More attention is paid to the analysis of the formation of the wave field. A comparison with the discrete wavenumber computations for long periods is made. The effects of slight absorption are considered.

The terminology used in the seismic response analysis is introduced in the next section. Then, advantages and limitations of the application of the ray method to seismic response analysis are discussed. The frequency-domain approach to the computation of the seismic response for slight-

ly absorbing media is then described. In principle, any available model of causal absorption, e.g. Futterman (1962), Kjartansson (1979), Mueller (1983), can be considered. Here, Futterman's causal model is adopted. An algorithm of the seismic response computations is described and results of computations are presented. *SH*-wave ray synthetic seismograms are evaluated on the free surface of the sedimentary basin assuming a vertical plane wave incident from below. The synthetics are compared with the results of other methods (discrete wavenumber method, glorified optics, finite-element and finite-difference methods). Various features of the computed wave field are explained in detail with the use of the decomposition of the wave field into elementary seismograms of individual multiples and by inspecting their rays. The limits of applicability of the ray method in low-frequency response computations are partially studied by comparing ray synthetics with discrete wavenumber synthetics. Finally, the effect of slight Futterman's causal absorption on ray synthetics for different degrees of absorption is shown.

Let us note that some preliminary results have been published in Moczo et al. (1986).

Seismic response of local structures

Seismic response analysis (or analysis of seismic mobility) of a certain local structure should involve an analysis of the transfer properties of the structure itself and an analysis of responses to a set of signals that are supposed to represent possible excitations of the structure during an earthquake. From this point of view, the seismic response of the local structure may be defined as a set of four characteristics of seismic ground motion: namely, an impulse response, a frequency response, a time history of a response and a Fourier spectrum of the time history of the response. If the structure is excited by Dirac δ-impulse, the generated vibration of the structure is the impulse response. The Fourier spectrum of the impulse response is the frequency response (spectral characteristics, transfer function). Often, the modulus of the frequency response is used as the frequency response. Both the impulse response and the frequency response only depend upon the properties of the structure (for a given type of wave, angle of incidence, azimuth), i.e., they only characterize the transfer properties of the structure. In practical computations, it is of no use to consider higher frequencies that are not important from the point of view of engineering seismology. Removing the high frequencies, we obtain a pseudo-impulse response. If the structure is excited by an arbitrary signal having a finite effective width of the spectrum, the generated vibration of the structure is the time history of the response. Instead of the complex Fourier spectrum of the time history, the amplitude Fourier spectrum is more often used.

Application of the ray method in seismic response analysis – advantages and limitations

Let us mention the most important aspects of the application of the ray method in seismic response analysis. The ray method is relatively fast and inexpensive. It is applicable to laterally inhomogeneous, possibly absorbing media with a complex surface and subsurface topography, layered and block structure, and an arbitrary distribution of velocities and density inside layers. The wave field may be generated by an incoming wave with an arbitrary curved wavefront, incident from an arbitrary direction on the bottom of the investigated structure. Any high-frequency source-time function can be used.

In the ray method, the wave field is decomposed into elementary waves. Thus, individual waves forming the seismic response may be identified, no matter whether the waves form an interference group or not. This enables the computed wave field to be decomposed and its physical nature to be better understood. It is possible to estimate the importance of individual elementary waves such as refracted, reflected, multiply reflected, converted waves. The ray method enables us to investigate the physical nature of wave groups with large amplitudes which may be caused, for example, by constructive interference or focusing effects. Since for each wave, rays are traced through the structure, it is easy to detect the interfaces or regions which are responsible for generating local effects. From the point of view of a possible decomposition of the computed wave field, the ray method is very useful even if the seismic response is computed by other methods such as finite-difference or finite-element methods that only yield the complete wave field. The interpretation of the complete wave field computed by these methods can be complicated even in relatively simple structures.

The ray method is a high-frequency method. It is applicable if the prevailing wavelength of considered signals is substantially smaller than any characteristic quantity of the length dimension (e.g., radius of curvature of boundaries including the free surface, measure of spatial changes of velocity, density, impedance, etc.), see Červený et al. (1977). As is shown later, the ray method can give reasonable results even if the above conditions are not strictly satisfied. In the high-frequency range, the ray method can complement the computations by other methods which are more effective for models whose dimensions are of the order of several wavelengths (finite differences) or, in principle, low-frequency methods (discrete wavenumber method). The ray method is especially important at those sites where only the study of high-frequency propagation has a practical meaning.

Since the number of elementary waves in the decomposition of the wave field may be infinite, only a finite number of the most important waves is considered in the ray method. Thus, the ray method does not generally give the complete wave field. Moreover, the computed wave field does not contain some types of waves, e.g. diffracted waves or so-called non-ray waves. For this reason, the ray method does not provide good results in such structures in which intense diffracted or non-ray waves are generated. For example, for diffracted waves caused by topographical anomalies see Zahradník and Urban (1984). Certain types of diffracted waves can be included in the computations if generalizations of the ray method, such as the edge wave method (Klem-Musatov and Aizenberg, 1984) or Gaussian beam method (Červený, 1985a), are used.

The ray method may be less effective if a large number of rays is required, especially rays which are reflected many times inside the structure. Such a situation may arise, for example, in the computation of the seismic response of a sedimentary basin with a very large impedance contrast between sediments and the underlying rocks.

The ray method does not work properly or even fails in singular regions, such as a caustic region, critical region

or transition from shadow to illuminated region. The ray amplitudes are infinite at caustics, and they are not accurate enough in the vicinity of caustics. This problem could be removed, for example, by applying the Gaussian beam method. The caustic may, however, be simply detected in the computed ray field and taken into account in the interpretation of the computed results. In applications, the problems connected with the existence of caustics can be avoided simply by slightly shifting the receiver from the caustic location on the surface, as suggested by Hong and Helmberger (1978) and used, for example, by Lee and Langston (1983b).

Computation of the seismic response of slightly absorbing structures

The so-called Debye procedure (see Kravtsov and Orlov, 1980; Červený, 1985a), and Futterman's model of causal absorption (see Futterman, 1962) are used to describe the behaviour of high-frequency seismic waves in laterally inhomogeneous slightly absorbing media. In absorbing media, Lamé's parameters λ and μ are complex-valued quantities:

$$\lambda=\lambda_R-\mathrm{i}\lambda_I, \qquad \mu=\mu_R-\mathrm{i}\mu_I. \tag{1}$$

In slightly absorbing media, λ_I and μ_I are small quantities. They are formally considered to be of order ω^{-1} for $\omega\to\infty$. Let us insert the parameters (1) into the elastodynamic equation and seek its approximate solution in the form

$$\mathbf{u}=\mathbf{U}\exp[-i\omega(t-\tau)]. \tag{2}$$

Here $\mathbf{U}$ is a complex-valued vectorial amplitude, τ is the phase function (eikonal), and ω and t are frequency and time. We do not repeat the whole procedure of determining $\mathbf{U}$ and τ since it is very similar to that used for perfectly elastic media (see Červený and Ravindra, 1971; Červený and Hron, 1980; Kravtsov and Orlov, 1980). We pay attention only to those steps in the procedure in which it differs from the procedure for perfectly elastic media.

Inserting Eq. (2) into the elastodynamic equation yields the basic system of equations of the ray method (Červený, 1985a, Section 2.3). Since λ_I and μ_I are of order ω^{-1}, they do not appear in the first equation from which the eikonal equations are obtained:

$$(\nabla\tau)^2=\rho/(\lambda_R+2\mu_R) \tag{3a}$$

for P waves, and

$$(\nabla\tau)^2=\rho/\mu_R \tag{3b}$$

for S waves. In Eq. (3), ρ denotes density.

Because of the complexity of Lamé's parameters, we also have complex-valued velocities $\alpha=\alpha_R-i\alpha_I$ and $\beta=\beta_R-i\beta_I$ of P and S waves propagating in a slightly absorbing medium. As for perfectly elastic media, we use the notation

$$\alpha^2=(\lambda+2\mu)/\rho, \qquad \beta^2=\mu/\rho, \tag{4}$$

from which we get

$$(\lambda_R+2\mu_R)/\rho=\alpha_R^2-\alpha_I^2, \qquad \mu_R/\rho=\beta_R^2-\beta_I^2, \tag{5a}$$

$$(\lambda_I+2\mu_I)/\rho=2\alpha_R\alpha_I, \qquad \mu_I/\rho=2\beta_R\beta_I. \tag{5b}$$

It follows from Eq. (5b) that α_I and β_I are of order ω^{-1}, like λ_I, μ_I. Neglecting terms of second order in ω^{-1}, we may therefore write the eikonal equation, Eq. (3), in the form

$$(\nabla\tau)^2=v_R^{-2}, \tag{6}$$

where v_R stands for either α_R or β_R. Thus, the rays in slightly absorbing media are real and may be constructed in the very same way as in perfectly elastic media (see Červený et al., 1977) with local velocities of P and S waves, α_R and β_R.

Let us now investigate the second basic equation of the ray method, which yields the transport equation. The second basic equation for slightly absorbing media has the form

$$\mathbf{M}(\mathbf{U};\lambda_R,\mu_R)+\omega[(\lambda_I+\mu_I)\nabla\tau(\mathbf{U}\nabla\tau)+\mathbf{U}\mu_I(\nabla\tau)^2].$$

For the term $\mathbf{M}(\mathbf{U};\lambda_R,\mu_R)$, see Červený (1985a) Eq. (2.11), in which λ,μ should be substituted by λ_R,μ_R. Thus, the second basic equation of the ray method for slightly absorbing media differs from the equation for perfectly elastic media by the term

$$\omega[(\lambda_I+\mu_I)\nabla\tau(\mathbf{U}\nabla\tau)+\mathbf{U}\mu_I(\nabla\tau)^2]\sim 2\rho\omega\mathbf{U}v_R^{-1}v_I.$$

The transport equation then has the form

$$2\rho v_R\,dU_i/ds+\rho v_R U_i\,d[\ln(J\rho v_R)]/ds+2\rho\omega U_i v_R^{-1}v_I=0. \tag{7}$$

Here, the components of the vectorial amplitude, U_i, are taken in the ray-centred coordinate system. The ray-centred coordinate system is an orthogonal system, two basis vectors of which are mutually perpendicular in the plane perpendicular to the ray. The third vector is tangent to the ray. The quantity J is the Jacobian of the transformation from the ray to the Cartesian coordinates. For details and methods of the determination of the ray-centred coordinate system and J, see Červený (1985a). The quantities v_R and v_I stand for α_R, α_I or β_R, β_I, s is an arclength along the ray.

The solution of Eq. (7) gives

$$\mathbf{U}=\boldsymbol{\Psi}(Jv_R\rho)^{-1/2}\exp\left(-\omega\int_{s_0}^{s}v_R^{-2}v_I\,ds\right), \tag{8}$$

the exponential term describing the decay of the amplitude due to a slight absorption along the ray path from s_0 to s. $\boldsymbol{\Psi}$ is a vector constant along the ray. Inserting Eq. (8) into Eq. (2), we get

$$\mathbf{u}=\boldsymbol{\Psi}(Jv_R\rho)^{-1/2}\cdot\exp\left[-i\omega t+i\omega\int_{s_0}^{s}v_R^{-1}(1+iv_Iv_R^{-1})\,ds\right]. \tag{9}$$

The integrand of Eq. (9) in our approximation (i.e. neglecting terms of higher order in ω^{-1}) is equal to the reciprocal value of the complex velocity,

$$v^{-1}=v_R^{-1}(1+iv_Iv_R^{-1}). \tag{10}$$

We now assume the frequency dependence of v, and thus v_R and v_I, to be expressed by Futterman's relations

$$v^{-1}(\omega)=v_R^{-1}(\omega)[1+i/(2Q(\omega))], \tag{11}$$

$$v_R^{-1}(\omega)=v_R^{-1}(\omega_r)\{1-[1/(\pi Q(\omega_r))]\ln(\omega/\omega_r)\}, \tag{12a}$$

$$Q(\omega)=Q(\omega_r)\{1-[1/(\pi Q(\omega_r))]\ln(\omega/\omega_r)\}, \tag{12b}$$

where ω_r is a reference frequency.

Comparing Eq. (10) with Eq. (11), we get

$$Q^{-1}(\omega)=2v_I(\omega)/v_R(\omega), \tag{13}$$

i.e. the reciprocal value of the quality factor Q is a quantity of the order ω^{-1}. From Eq. (12) immediately follows

$$v_R(\omega)\,Q(\omega)=v_R(\omega_r)\,Q(\omega_r), \tag{14}$$

i.e. the product $v_R Q$ is independent of the frequency. Let us assume that we know the velocity and Q distribution for the reference frequency ω_r. Then the integrand of Eq. (9) may be rewritten, by using Eqs. (12)–(14), in the form

$$\begin{aligned} &v_R^{-1}(\omega)+\frac{i}{2}Q^{-1}(\omega)\,v_R^{-1}(\omega)\\ &=v_R^{-1}(\omega_r)[1-\pi^{-1}Q^{-1}(\omega_r)\ln(\omega/\omega_r)]\\ &\quad+\frac{i}{2}Q^{-1}(\omega_r)\,v_R^{-1}(\omega_r). \end{aligned} \tag{15}$$

For the term $v_R(\omega)$ under the square root in Eq. (9) we may write

$$v_R(\omega)\sim v_R(\omega_r), \tag{16}$$

since the second term in Eq. (12a) would produce an additional amplitude term of the order ω^{-1}. In the following, we consider only one component of $\mathbf{u}$ in an arbitrary orthogonal coordinate system. For simplicity, we denote this component u. Similarly, Ψ is the corresponding component of $\boldsymbol{\Psi}$. Since the term $\Psi(Jv_R\rho)^{-1/2}$ is generally complex valued, we can rewrite it as follows:

$$\Psi(Jv_R\rho)^{-1/2}=A\exp(i\chi). \tag{17}$$

Inserting Eqs. (15)–(17) into Eq. (9), we get

$$u=A\exp\left\{-\frac{1}{2}\omega t^*-i\omega\left[t-\tau+\frac{t^*}{\pi}\ln(\omega/\omega_r)\right]+i\chi\right\}, \tag{18}$$

where $\tau=\int_{s_0}^{s} v_R^{-1}(\omega)\,ds$ and $t^*=\int_{s_0}^{s}[v_R(\omega_r)\,Q(\omega_r)]^{-1}\,ds$ are the travel time and the global absorption factor. Let us note that for $\omega<\omega_r$, $t^*\pi^{-1}\ln(\omega/\omega_r)<0$, i.e. the travel time is greater for a lower frequency, and vice versa, which is in agreement with the causality principle.

Expression (18) represents a contribution of one elementary wave. In the ray method, the resulting wave field u^T is a superposition of all elementary waves arriving at a receiver: $u^T=\sum_k u^k$, where u^k is the contribution (18) of the k-th elementary wave. From u^T we immediately get the frequency response of the structure

$$\begin{aligned} U^T(\omega)=&\sum_k A_k\exp(-\tfrac{1}{2}\omega t_k^*)\\ &\cdot\exp\left\{i\left[\chi_k-\frac{\omega}{\pi}t_k^*\ln(\omega/\omega_r)+\omega\tau_k\right]\right\}. \end{aligned}$$

In the case of a perfectly elastic medium, $t^*=0$ and

$$U^T(\omega)=\sum_k A_k\exp[i(\chi_k+\omega\tau_k)].$$

In both cases, the fast frequency response algorithm (see Červený, 1985b) can be used for an effective evaluation of the frequency response.

The impulse response is the inverse Fourier transform of the frequency response. Undesired high frequencies greater than $\omega=\omega_{\max}$, can be removed by a smoothing filter $W(\omega)$: $W(\omega)=0$ for $|\omega|>|\omega_{\max}|$, $U^W(\omega)=U^T(\omega)\,W(\omega)$. Applying the inverse Fourier transform to $U^W(\omega)$, we obtain the pseudo-impulse response. A response $R(\omega)$ of the structure to a signal $s(t)$ with the spectrum $S(\omega)$ is $R(\omega)=S(\omega)\,U^W(\omega)$ in the frequency domain. Applying the inverse Fourier transform to $R(\omega)$, we obtain the time history of the response corresponding to $s(t)$.

The above approach to the computation of the seismic response, in which the frequency response is computed from travel times, amplitude moduli, phase shifts and global absorption factors, represents the frequency-domain approach.

An alternative to this approach is the time-domain approach. In this case we obtain from (18)

$$\begin{aligned} u=A\exp(i\chi)\frac{1}{\pi}\int_0^\infty S(\omega)\exp\Big[&-\frac{1}{2}\omega t^*-i\frac{\omega}{\pi}t^*\ln(\omega/\omega_r)\\ &-i\omega(t-\tau)\Big]d\omega, \end{aligned} \tag{19}$$

where $S(\omega)$ is the spectrum of the source-time function $s(t)$. Let us denote

$$F(\omega)=S(\omega)\exp\left[-\frac{1}{2}\omega t^*-i\frac{\omega}{\pi}t^*\ln(\omega/\omega_r)\right],$$

$$\frac{1}{\pi}\int_0^\infty F(\omega)\exp(-i\omega\vartheta)\,d\omega=\hat{\mathbf{f}}(\vartheta)+i\hat{\mathbf{g}}(\vartheta), \tag{20}$$

where $\vartheta=t-\tau$. Then, for the real part of Eq. (19) we can write

$$\operatorname{Re} u=A[\hat{\mathbf{f}}(\vartheta)\cos\chi-\hat{\mathbf{g}}(\vartheta)\sin\chi]. \tag{21}$$

Here, as can be seen from Eq. (20), $\hat{\mathbf{g}}(\vartheta)$ is the Hilbert transform of $\hat{\mathbf{f}}(\vartheta)$. Equation (21) corresponds to one elementary wave and it is the well-known formula for an elementary seismogram in the zero-order approximation of the ray method. However, $\hat{\mathbf{f}}(\vartheta)$ in Eq. (21) is not the source-time function since $\hat{\mathbf{f}}(\vartheta)$ includes the effect of absorption. The resulting wave field $\operatorname{Re} u^T$ will be a superposition of all elementary waves: $\operatorname{Re} u^T=\sum_k \operatorname{Re} u^k$, where

$$\operatorname{Re} u^k=A_k[\hat{\mathbf{f}}_k(\vartheta_k)\cos\chi_k-\hat{\mathbf{g}}_k(\vartheta_k)\sin\chi_k]. \tag{22}$$

$\operatorname{Re} u^T$ represents the time history of the response of the structure to the signal $s(t)$.

Thus, it is possible to choose between the two approaches. In the time-domain approach it is necessary to evaluate the inverse Fourier transform in the computation of each elementary wave, see Eqs. (20)–(22). In the frequency-domain approach it is sufficient to evaluate the inverse Fourier transform only once. Moreover, once the fre-

quency response has been evaluated, it is easy to compute time histories for different source-time functions. The frequency-domain approach is therefore more convenient (faster) than the time-domain approach. The time-domain approach could be convenient in the case of the computation of time histories of the responses to special analytical signals, like Gabor signal, for which simple approximate formulae for their Hilbert transform and for elementary seismograms are derived, see Červený (1976) and Červený and Frangié (1980, 1982).

A short description of program package RESPO

Program package RESPO (Moczo et al., 1985) is designed for the computation of the seismic response on the free surface of $2-D$ laterally inhomogeneous geologic structures assuming *P*, *SV* or *SH* plane-wave incidence from below. The basic part of package RESPO is a modified version of the main program of package SEIS83 (Červený and Pšenčík, 1984). The algorithm of the computation of the wave field is based on the zero-order approximation of the ray method. The computation is performed in two steps. In the first step, rays, travel times, complex-valued ray amplitudes and global absorption factors of individual elementary waves (e.g. direct, multiply reflected/refracted waves) are computed by program SEIM and stored. In the second step, four characteristics of the seismic response (mentioned earlier) may be computed in program FSYNT from the quantities stored in SEIM. The frequency-domain approach is used. Let us mention that such a "two-step approach" to the computation of the seismic response, which includes the computation of the impulse response in the first step, has been suggested for finite-difference computations by Zahradník and Urban (1984).

Two-dimensional, laterally inhomogeneous, possibly absorbing layered structures with curved interfaces and a free surface, including block structures, vanishing layers and isolated bodies, can be considered. The interfaces may be specified by a system of points and then approximated by cubic splines or approximated by analytic formulae. Within a layer, the velocity distribution is specified at grid points of a rectangular network and then approximated by bicubic spline interpolation. It is possible to specify several Q-factor distributions for one velocity model and to compute corresponding global absorption factors along each ray. Non-causal absorption, as well as various models of causal absorption (Futterman, 1962; Kjartansson, 1979; Mueller, 1983), may be considered.

The angle of incidence of the incident plane wave may be arbitrary. *P*, *SV*, *SH* and converted waves may be computed. The rays arriving at specified receivers are computed by boundary-value ray tracing based on shooting. The same procedure as in Červený and Pšenčík (1984) is used for this purpose. The amplitudes are evaluated by standard ray formulae. In the case of an *S* wave, the *SV* and *SH* ray amplitude components are evaluated simultaneously.

Once rays, travel times, complex-valued amplitudes and global absorption factors are evaluated, an arbitrary number of responses for various types of exciting signals can be computed. As the exciting signal, an analytic impulse or an arbitrary digitized seismic record may be used, no matter whether it corresponds to a seismic displacement, velocity or acceleration. Selections of receivers and elementary waves are possible. A more detailed description of package RESPO can be found in Moczo et al. (1985).

Numerical examples

Comparison of ray computations with other computations for a perfectly elastic medium

SH ray synthetic seismograms at the free surface of a sedimentary basin excited by a vertically incident plane *SH* wave were computed. The model of the basin (see Fig. 1) had been studied by Boore et al. (1971) and subsequently by many authors using various methods. The seismograms presented here were computed by program package RESPO.

Figure 2 shows a comparison of synthetic seismograms evaluated by five different methods: (1) ray method calculations by RESPO, (2) discrete wavenumber method by Bard and Bouchon (1980), (3) glorified optics method by Hong and Helmberger (1978), (4) finite-element method by Hong and Kosloff, see Hong and Helmberger (1978), (5) finite-difference method by Boore et al. (1971). Seismograms 2–5 are taken from Bard and Bouchon (1980).

Since 1980 several other authors have computed seismograms for the basin model. Let us mention Virieux (1984), who computed seismograms up to 180 s with velocity-stress finite-difference method, and Kohketsu (1987), who used the $2-D$ reflectivity method for the same model. The agreement of the ray method results with the results of the last two mentioned authors seems to be quite good, at least for shorter times.

Besides the direct wave, our computation includes the waves multiply reflected inside the basin. The multiples are classified by the number of reflections from the basin bottom. Multiples with up to a maximum of ten reflections from the bottom are considered.

The basin was successively illuminated by the direct wave, once-reflected wave, etc., up to the 10-times-reflected

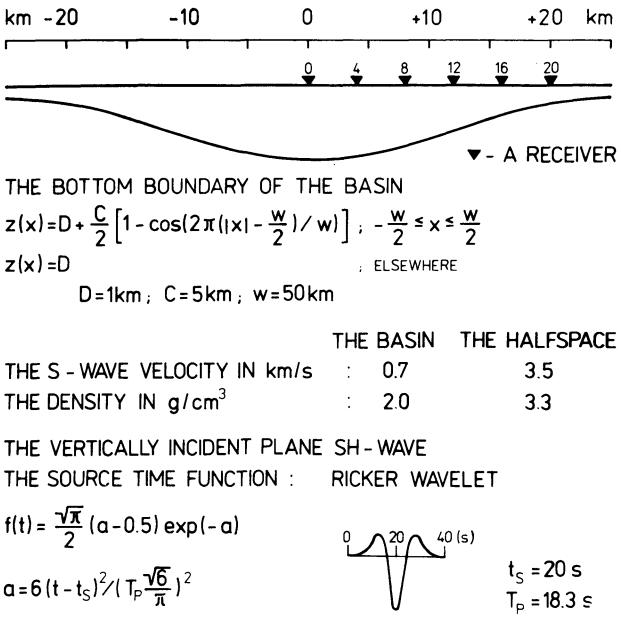

Fig. 1. Description of the basin model and the exciting wave. The maximum depth of the basin is 6 km

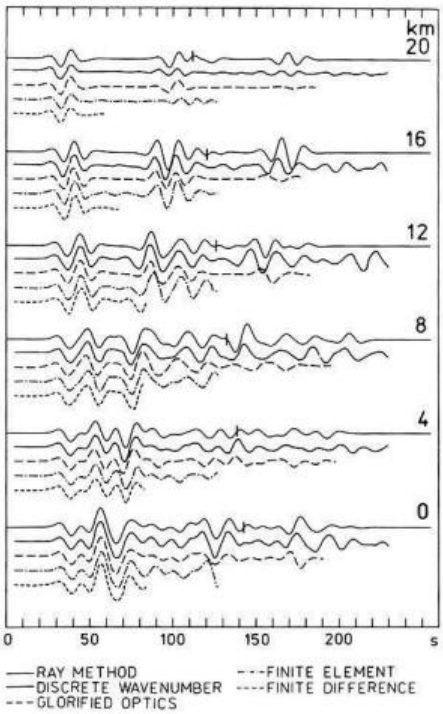

Fig. 2. Comparison of *SH* synthetic seismograms computed by ray (program package RESPO), discrete wavenumber (Bard and Bouchon, 1980), glorified optics (Hong and Helmberger, 1978), finite-element (Hong and Kosloff) and finite-difference (Boore et al., 1971) methods for the basin model shown in Fig. 1

wave. The higher the multiple, the greater the number of rays forming the multiple. Because of the symmetry of the basin, it was sufficient to illuminate only one-half of the basin. The results of the boundary-value ray tracing were carefully checked in order to obtain all rays arriving at the receivers.

Due to the missing multiples of higher order than 10, the later parts of the seismograms can be distorted. Time intervals that should not be distorted by missing higher multiples are marked by vertical bars (confidence bars) in Fig. 2. The determination of confidence bars can be demonstrated on the frame for the receiver at 20 km in Fig. 3a. We can see that the seismograms of individual multiples form three nearly vertical branches. We do not expect the first branch to become stronger for higher multiples than those shown. Therefore, we define the confidence bar by the arrival time of the fastest ray of the 10-times-reflected multiple contributing to the second branch. In this way, for the receiver at 20 km we get a confidence bar at about 112 s. Confidence bars are frequency independent in perfectly elastic media. They shift to larger arrival times when absorption is considered, see Fig. 3b.

We have to take confidence bars into consideration when comparing the seismograms in Fig. 2. At shorter times, the agreement of all five computations is very good. At later times, some differences occur. Let us point out the especially good agreement of ray results with the discrete wavenumber results. Somewhat surprisingly, there are certain differences between the glorified optics and our results. A partial explanation is that the glorified optics method does not involve 10-times-reflected waves. However, the absence of these waves cannot fully account for the differences. This may be seen, for example by comparing the interval 160–180 s on seismograms for the basin centre in Fig. 2 and seismograms of multiples presented in Fig. 3a. In this time interval the strongest contributor is the 8-times-reflected wave. Possible explanation of discrepancies in later arrivals are incorrect phase shifts caused by caustics in the glorified optics method.

There is disagreement in amplitudes between the ray and discrete wavenumber synthetics at their ends for receivers at 16 and 20 km, see Fig. 2, which is probably caused by missing higher multiples in the ray computations. The corresponding wave groups are due to interference of a large number (several tens) of contributors with comparable amplitudes. Only two of all contributors in the 9-times-reflected wave at the receiver at 20 km are stronger due to geometrical focusing.

Decomposition of the wave field into contributors along rays

In order to understand the formation of the wave field, let us investigate the seismograms of multiples and their rays separately.

Individual lines in Fig. 3a show, starting from the top, the seismograms of the direct wave (*D*), the once-reflected wave (1), etc. for receivers at 0, 4, 8, 12, 16 and 20 km. The seismograms at the bottom are superpositions of all the above elementary seismograms. Short vertical lines again denote confidence bars. In Fig. 3a, a perfectly elastic medium is considered. The seismograms in Fig. 3b correspond to an absorbing medium and are discussed later.

Three nearly vertical branches may be clearly seen on seismograms of multiples at receiver positions 12, 16 and 20 km in Fig. 3a. These branches correspond to three clearly separated wave groups in synthetics.

An inspection of the rays arriving at the receiver at 12 km shows the following. The first branch (20–65 s) corresponds to rays entering the basin on the right of the receiver, travelling between the basin bottom and the free surface and arriving at the receiver from the right after the respective number of reflections. An example of rays of this type is the 8-times-reflected ray shown in Fig. 4a. The second branch (65–140 s) corresponds to rays (see Fig. 4b) entering on the opposite (left) side of the basin, travelling across the basin and arriving at the receiver from the left (ray 2 in Fig. 4b). Some rays travel to the right of the receiver, where they are reflected to the opposite direction and finally arive at the receiver from the right (ray 3 in Fig. 4b). The third branch (140–200 s) corresponds to rays (see Fig. 4c) entering on the right side of the basin, travelling across the basin, reflected on the left side of the basin, again travelling across the basin and arriving at the receiver. As in the second branch, some rays arrive at the receiver from the left (ray 4 in Fig. 4c), other rays travel to the right of the receiver, where they are reflected to the opposite direction and finally arrive at the receiver from the right (ray 5 in Fig. 4c).

Practically the same holds for the receiver position at 20 km. The branches are, however, better separated in time and the rays similar to ray 5 in Fig. 4c are not present. They would probably appear in higher multiples. The examples of the rays of the 8-times-reflected wave arriving at the receiver at 20 km are shown in Fig. 5.

The form of the seismograms at receiver positions 0, 4 and 8 km is more complicated. At 0 km, there are four branches in seismograms. They are marked by lines 1–4

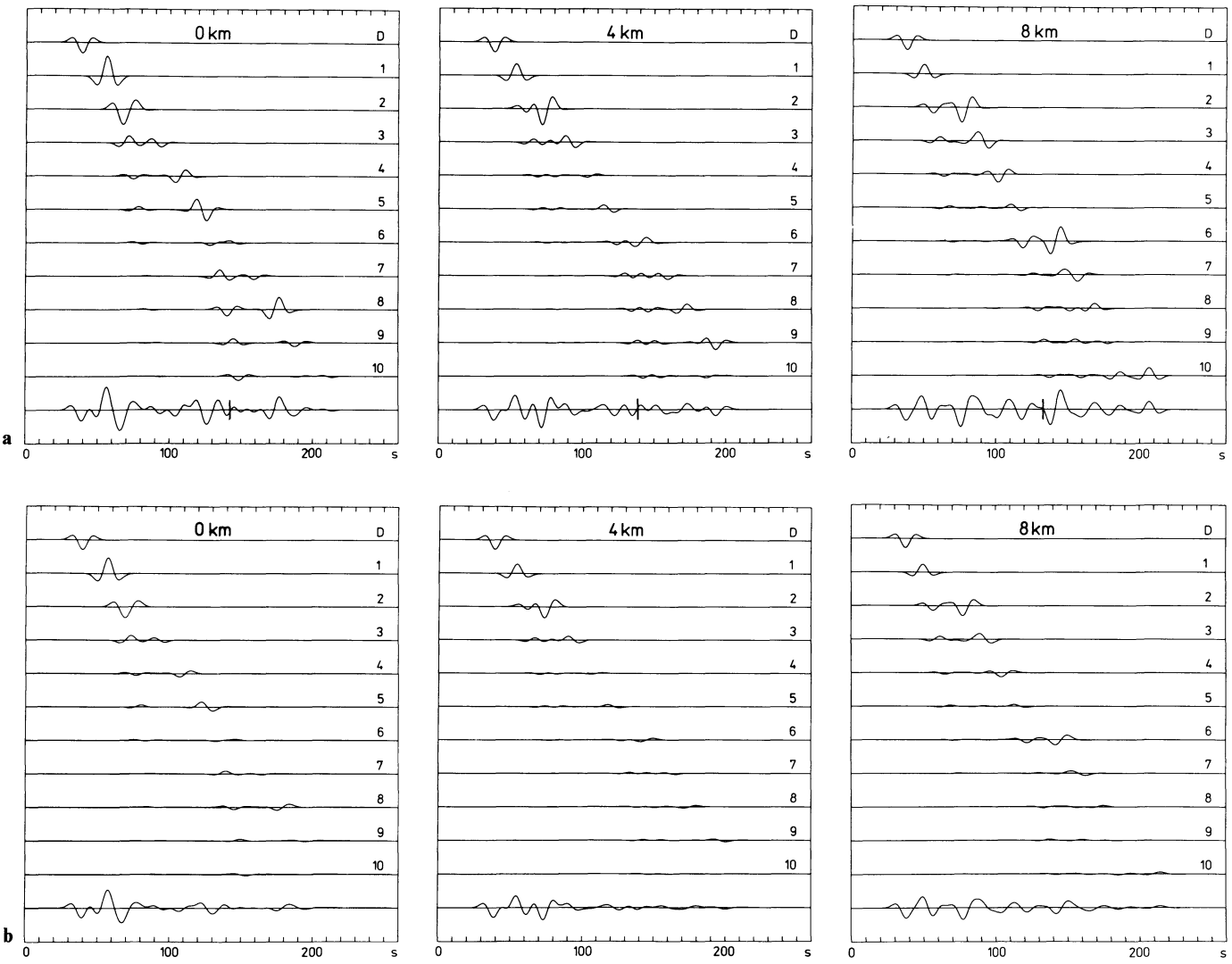

Fig. 3a, b. Elementary seismograms of multiples: **a** without absorption; **b** with Futterman's causal absorption, $Q=20$ at 1 Hz. *D* denotes the direct wave, *1* – the wave reflected once from the bottom of the basin, *2* – the wave reflected twice from the bottom of the basin, etc. The synthetic seismograms (shown also in Fig. 2) *at the bottom of each frame* are superpositions of all the above elementary seismograms

in Fig. 6a. Since the receiver is situated at the symmetry axis of the basin, there are, with the exception of the rays normally incident at the receiver, always two rays which arrive symmetrically at the receiver. In Fig. 6c–e, only one of these rays is fully depicted (denoted by *R*); of the other one (denoted by *L*), only the incident part is shown. Line 1 in Fig. 6a corresponds to rays propagating along the vertical axis of symmetry of the basin, see Fig. 6b. Line 2 corresponds to rays entering on one side of the basin, travelling between the basin bottom and the free surface and arriving after the respective number of reflections at the receiver. Figure 6c gives such an example for a ray corresponding to the 8-times-reflected wave. Line 3 corresponds to rays entering on one side of the basin, travelling to the opposite side, reflecting there and arriving at the receiver, see Fig. 6d. Line 4 corresponds to rays that travel only in that part of the basin where the depth is greater than roughly half the maximum depth. (It corresponds approximately to the range interval from -14 to $+14$ km.) These rays do not reach the margins of the basin and they are reflected on both slopes of the basin. Some of them propagate almost vertically in the narrower central part of the basin. An example is shown in Fig. 6e.

There is a slightly different situation at the receiver at 4 km, see Fig. 3a. Since the receiver is not at the symmetry axis of the basin, branches 2 and 3 from the previous case (see Fig. 6a) are split into two sub-branches. One subbranch corresponds to rays entering on the left side of the basin, the other to rays entering on the right side. There are no rays propagating strictly along the vertical axis, as in the case of the receiver at 0 km. Thus, the maximum travel times in each multiple correspond to the rays propagating almost vertically in the narrow central part of the basin and, in the case of higher multiples, also to the rays that travel inside that part of the basin corresponding approximately to the range interval from -15 to $+15$ km and are reflected on both slopes of the basin.

Let us mention several general features of rays and contributions connected with them. The higher the multiple, the greater the number of rays forming this multiple at a receiver. The rays with almost vertical elements often become weak contributors after several reflections (small re-

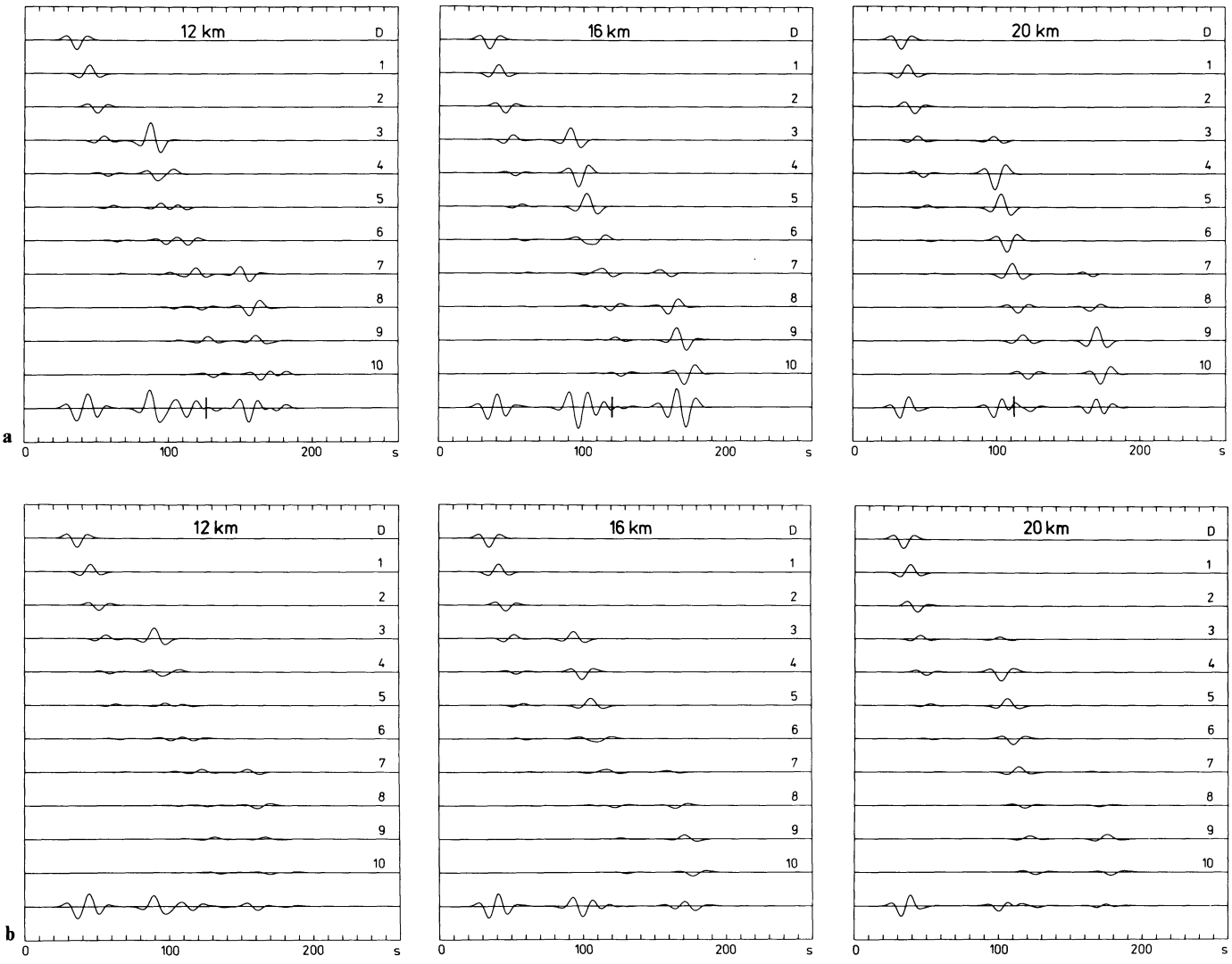

Fig. 3 (cont.)

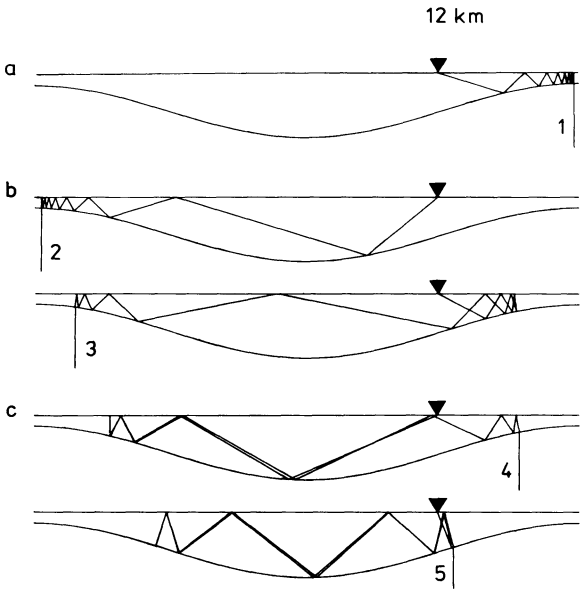

Fig. 4a–c. Examples of various types of rays, 8-times reflected from the basin bottom and arriving at the receiver position at 12 km

flection coefficients). This is different for the vertically propagating rays at the centre of the basin. They are relatively strongly focused and thus the amplitude decrease due to reflections is partially compensated for by the focusing. The number of rays with nearly horizontal elements between the left and right margins of the basin is higher than those with nearly vertical elements. Most of these rays are overcritically reflected. Thus, the decrease in their amplitudes due to reflections is negligible. The amplitudes connected with these rays, however, are often decreased by a large geometrical spreading.

An inspection of the rays corresponding to the seismograms in Fig. 3a (all shown in Fig. 7) suggests the following explanation of the resultant synthetics. The waves corresponding to the rays entering the basin on the right margin and travelling (with a respective number of reflections) to the opposite side of the basin mutually interfere and form a local interference wave propagating from the right to the left margin of the basin (sometimes called local Love wave). Rays 1, 6 and 11 *R* shown in Figs. 4, 5 and 6, respectively, are examples of the rays of the waves forming this interference wave. This wave is denoted by line 1 in Fig. 7. Due to the symmetry of the problem, a similar interference wave

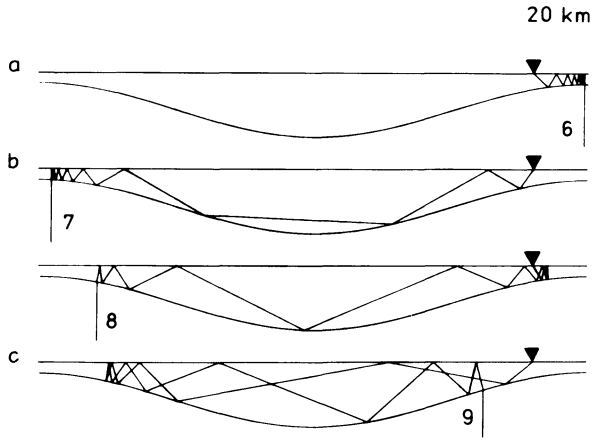

Fig. 5a–c. The same as in Fig. 4, but for the receiver position at 20 km

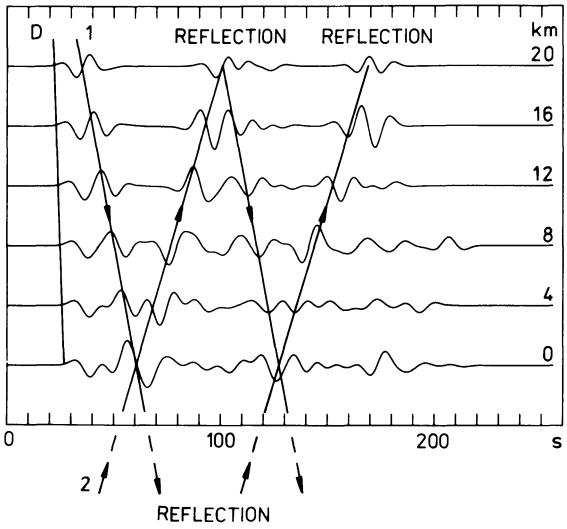

Fig. 7. Synthetic section with marked direct wave denoted by *D* and local interference waves propagating horizontally from the right *(left)* margin of the basin to the left *(right)* denoted by *1* (*2*). After reaching the opposite side of the basin, waves *1* and *2* are reflected back

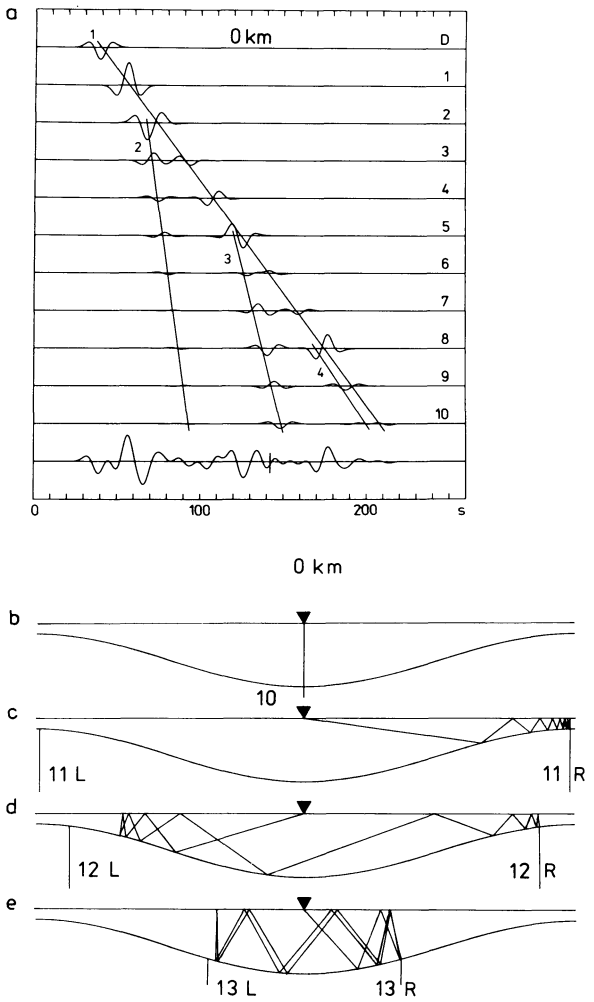

Fig. 6. a Formation of the wave field at the receiver at 0 km. Four branches formed by various waves propagating along various types of rays are denoted by numbers *1–4*. **b–e** Examples of 8-times-reflected rays; the rays incident on the left margin of the basin and denoted by *L* would have trajectories symmetrical to the rays incident on the right margin of the basin. The rays of type **b** contribute to line *1* in **a**; of type **c** to *2*; **d** to *3* and **e** to *4*

propagates from the left to the right margin (line 2). Examples of the corresponding rays are rays 2, 7 and 11 *L* in Figs. 4, 5 and 6, respectively. The interference waves meet at the centre of the basin. At the margins, the waves are reflected and propagate back to the side of their origin (rays 4, 9 and 12 *R* and rays 3, 8 and 12 *L*). There they are again reflected (ray 5 in Fig. 4 is an example).

A certain part of the elastic energy is focused in the central part of the basin and oscillates vertically between the bottom boundary and the free surface. Rays 10, 13 *R* and 13 *L* in Fig. 6 are examples.

Thus, we have two main types of wave propagation inside the basin: (1) the horizontally propagating local interference waves (local Love waves) that are observable at all receivers, see Fig. 7; (2) the vertically propagating wave that can be seen clearly in the seismograms of multiples for the receivers in the central part of the basin (0, 4 and 8 km), see Fig. 6a. It is evident from Fig. 7 that the horizontal wave propagation is dominant.

Comparison of ray and discrete wavenumber synthetics for long periods (low frequencies)

The agreement of the ray and discrete wavenumber synthetics in Fig. 2 may be surprising because of the simplicity and high-frequency character of the ray method. In the situation shown in Fig. 2, the prevailing wavelength λ_p of the incident wave is approximately twice as large as the maximum basin depth ($\lambda_p = 13$ km, and the depth at the centre of the basin is 6 km). The radii of curvature of the basin boundary are approximately 25, 93, 67 and 33 km at 0, 10, 16 and 20 km from the centre of the basin, respectively, i.e. larger than the prevailing wavelength of the incident wave. It is of interest to find out how accurate the ray synthetics are for wavelengths comparable with and larger than the radii of curvature. In the following, we present the results for prevailing wavelengths of about 28, 42 and 56 km (corresponding to prevailing periods of 40, 60 and

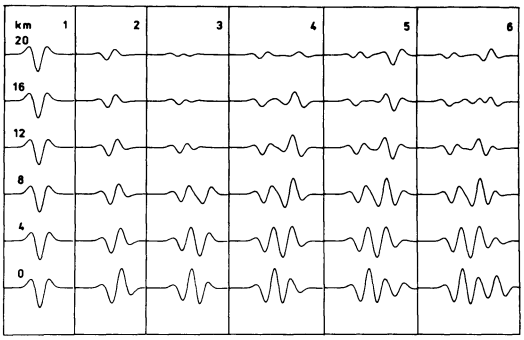

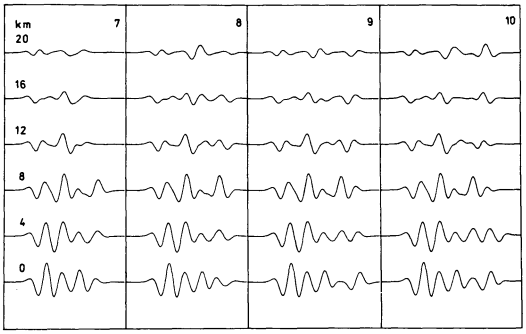

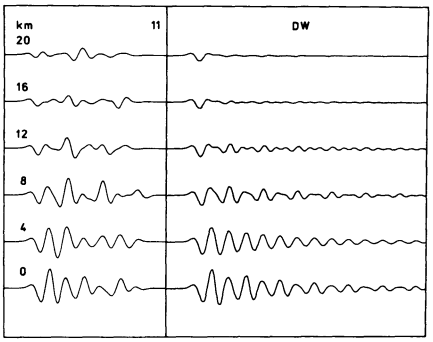

Fig. 8. Comparison of ray and discrete wavenumber synthetics for a prevailing wavelength of approximately 28 km ($T_p = 40$ s). The results of the discrete wavenumber method are denoted by *DW*. The synthetics with numbers are ray synthetics which include successively increasing numbers of multiples: *1* direct wave only, *2* superposition of the direct wave and once-reflected wave etc.

80 s). Since the discrete wavenumber method is a low-frequency method, the accuracy of its results is expected to be higher for these large wavelengths.

Eleven synthetics for $\lambda_p = 28$ km ($T_p = 40$ s) for each receiver are presented in Fig. 8. The synthetics with numbers are ray synthetics which include a successively increasing number of multiples: 1 corresponds to the direct wave only, 2 to the superposition of the direct and once-reflected waves etc., up to 11, which corresponds to the superposition of the direct wave and all the multiples up to the 10-times-reflected wave. DW denotes the discrete wavenumber results. The horizontal and vertical scales are the same for all seismograms in Figs. 8–10. Although the conditions of applicability of the ray method are not strictly satisfied, the ray results for the maximum number of multiples included (i.e. synthetics 11) resemble the results of the DW method, especially in the central part of the basin and for shorter times. In the central part of the basin, even the amplitudes of oscillations in both results differ only slightly.

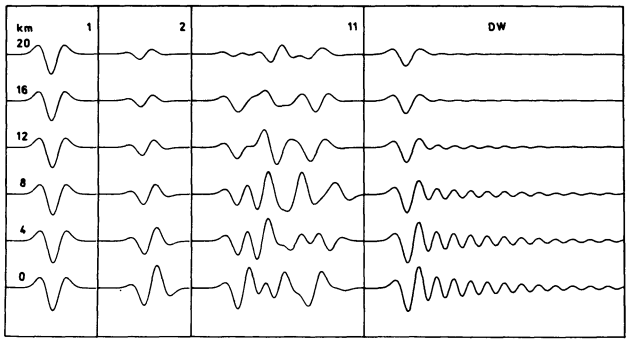

Fig. 9. The same as in Fig. 8, but for a prevailing wavelength of approximately 42 km ($T_p = 60$ s)

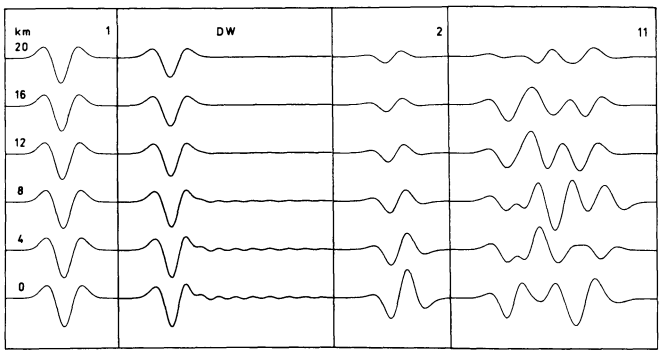

Fig. 10. The same as in Fig. 8, but for a prevailing wavelength of approximately 56 km ($T_p = 80$ s)

Figure 9 shows the ray synthetics 1, 2 and 11, and DW synthetics, for the prevailing wavelength 42 km ($T_p = 60$ s), i.e. nearly twice the minimum radius of curvature of the basin boundary. As expected, the discrepancies between the ray and DW synthetics are considerably greater than in the previous case.

Finally, Fig. 10 shows the synthetics for the prevailing wavelength 56 km ($T_p = 80$ s). In this case, the ray synthetics including only the direct wave are comparable with DW synthetics. Addition of any number of higher multiples would yield worse results.

We can see that the concept of approximating the wave field by a superposition of multiply reflected waves propagating along the geometrical ray paths fails for wavelengths larger than the minimum radius of curvature of the basin boundary. For wavelengths comparable with the minimum radius of curvature and considerably larger than the depth of the basin, the concept already yields reasonably good results in the central part of the basin for shorter times. The relatively good fit between the direct wave and DW synthetics for the prevailing wavelength 56 km is probably a consequence of the lower sensitivity of such a long incident wave to the basin structure.

The above tests illustrate that the ray method can give good results even in those frequency ranges where it is not expected. The ray synthetics are, however, more accurate and more effective for higher frequencies, with which we deal in many applications. In Fig. 11, ray synthetics are shown for four different frequencies which correspond to prevailing wavelengths of 1.5, 3, 6 and 12 km (i.e. lower than and comparable with those in Fig. 2). The longest wavelength is approximately half the radius of curvature of

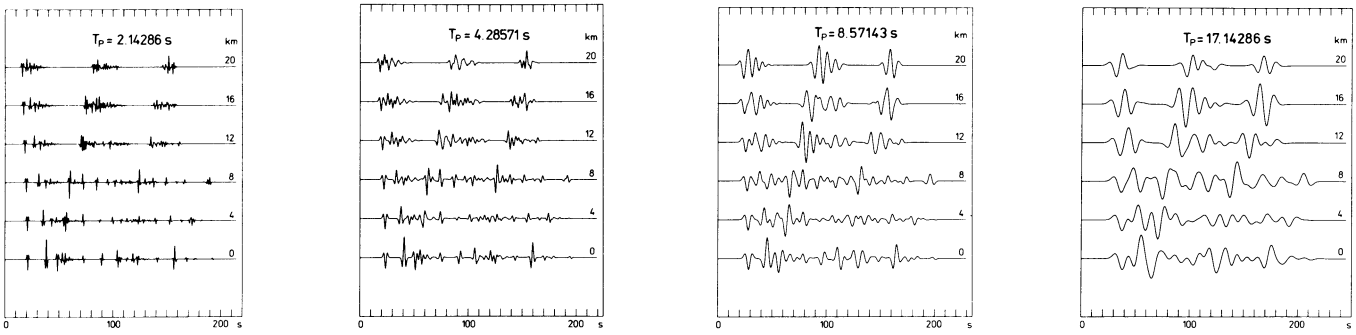

Fig. 11. The dependence of the ray synthetics on the prevailing period T_p. The corresponding prevailing wavelengths are 1.5, 3, 6 and 12 km

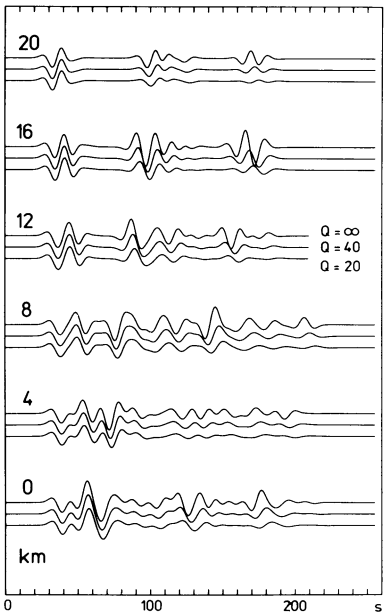

Fig. 12. The effect of Futterman's causal absorption. Comparison of the ray synthetics for three values of the quality factor Q: ∞ (perfect elasticity), 40, 20. The Q values are specified for 1 Hz

the basin boundary in its central part. It is interesting to see how the synthetics vary due to interference of contributors of various wavelengths.

Absorbing effects on the ray method synthetics

Figure 3b and Fig. 12 show the effect of the Futterman causal absorption on the ray synthetics. Only the absorption effects along a ray path are considered, the effects due to reflection/transmission (e.g. see Krebes, 1983) are omitted. The quality factor Q and velocity are specified for the frequency of 1 Hz. Figure 3b shows the seismograms of individual multiples and complete seismograms for $Q=20$. In Fig. 12, ray synthetics for $Q=\infty$ (perfectly elastic medium), $Q=40$ and 20 are shown. The prevailing wavelength is approximately 13 km in all cases. The decrease in amplitudes and the time delay are clearly seen at later times. Although the quality factor is relatively low, the decrease in the amplitudes due to absorption is not so expressive. This is due to the relatively large periods of the waves and relatively short travel times. Note that a similar result has been obtained by Zahradník and Urban (1984).

In the previous comparisons of the ray method with the discrete wavenumber method we have seen that the discrepancies between both methods were partially caused by not considering enough multiples. In models with absorption, the situation simplifies in this respect since the higher multiples are more attenuated (due to their longer travel paths) than the first onsets. Thus, it seems that the ray method is not only well suited for the computation in slightly absorbing media, but it may be even more adequate there.

Conclusion

A method of seismic response analysis of $2-D$ absorbing structures, based on the ray method, is presented. The frequency-domain approach to computing the seismic response has been chosen since it is more effective than the construction of ray synthetic seismograms by the summation of elementary seismograms (i.e. time-domain approach). Moreover, the frequency-domain approach allows simple recomputation of time histories for different source-time functions once the frequency response is known.

The computation of the seismic response is performed in two steps. In the first step, rays, travel times, complex-valued ray amplitudes and global absorption factors of individual elementary waves are computed. In the second step, four characteristics of the seismic response (the frequency response, impulse response, time history of the response, spectrum of the time history) are computed from travel times, complex-valued amplitudes and, if required, also from global absorption factors. Once we know these quantities, we can compute seismic responses for practically any high-frequency exciting signal.

SH ray synthetic seismograms have been computed on the free surface of the classical sedimentary basin assuming vertical *SH* plane-wave incidence. The synthetics were compared with synthetics computed by the discrete wavenumber, glorified optics, finite-element and finite-difference methods. Within the bars of confidence, especially good agreement has been found between the discrete wavenumber and ray method results.

A detailed inspection of individual elementary waves forming the seismograms and their rays revealed two main types of propagation inside the basin: the horizontally propagating local interference waves observable at all receivers, and the vertically propagating wave in the central part of the basin.

The comparison of ray synthetics with discrete wavenumber synthetics for wavelengths comparable with and

larger than the minimum radius of curvature of the basin boundary has shown the following. The concept of approximating the wave field by a superposition of multiply reflected waves with geometrical ray paths fails for wavelengths larger than the minimum radius of curvature of the basin boundary. For wavelengths comparable with the minimum radius of curvature and considerably larger than the depth of the basin, the concept yields reasonably good results in the central part of the basin for shorter times.

The effect of Futterman's causal absorption on the ray synthetics has also been demonstrated. It produces a decrease in amplitudes and time delays at later times.

Without doubt, the ray method is a useful tool in seismic response analysis. It can be applied to rather complicated, even slightly absorbing media and enables a detailed insight into the computed wave field. It is relatively fast and gives sufficiently accurate results, especially for higher frequencies. If waves reflected many times are to be computed (as they were in our study in the case of a perfectly elastic medium), it is advisable to use some new concepts like paraxial ray approximation to make the procedure more efficient. It would not be difficult to consider, instead of plane-wave incidence, incidence of a wave generated by a point source or even by an extended earthquake source and to study combined effects of the structure and the source.

Acknowledgements. The authors are greatly indebted to Prof. V. Červený and Dr. J. Zahradník for critical reading of the manuscript. We thank two anonymous reviewers for their helpful comments.

References

Bard, P.-Y., Bouchon, M.: The seismic response of sediment-filled valleys. Part 1. The case of incident *SH* waves. Bull. Seismol. Soc. Am. **70**, 1263–1286, 1980

Bard, P.-Y., Gariel, J.Ch.: The seismic response od $2-D$ sedimentary deposits with large vertical velocity gradients. Bull. Seismol. Soc. Am. **76**, 343–366, 1986

Boore, D.M., Larner, K.L., Aki, K.: Comparison of two independent methods for the solution of wave scattering problems: response of a sedimentary basin to vertically incident *SH* waves. J. Geophys. Res. **76**, 558–569, 1971

Červený, V.: Approximate expressions for the Hilbert transform of a certain class of functions and their application to the ray theory of seismic waves. Stud. Geophys. Geod. **20**, 125–132, 1976

Červený, V.: The application of ray tracing to the numerical modeling of seismic wavefields in complex structures. In: Handbook of Geophysical Exploration. Section I: Seismic exploration, K. Helbig and S. Treitel, eds., volume on Seismic shear waves, G. Dohr, ed.: pp. 1–124. London: Geophysical Press 1985a

Červený, V.: Ray synthetic seismograms for complex two-dimensional and three-dimensional structures. J. Geophys. **58**, 2–26, 1985b

Červený, V., Frangié, A.B.: Elementary seismograms of seismic body waves in dissipative media. Stud. Geophys. Geod. **24**, 365–372, 1980

Červený, V., Frangié, A.B.: Effects of causal absorption on seismic body waves. Stud. Geophys. Geod. **26**, 238–253, 1982

Červený, V., Hron, F.: The ray series method and dynamic ray tracing systems for $3-D$ inhomogeneous media. Bull. Seismol. Soc. Am. **70**, 47–77, 1980

Červený, V., Pšenčík, I.: SEIS83 – Numerical modeling of seismic wave fields in $2-D$ laterally varying layered structures by the ray method. In: Documentation of earthquake algorithms, Report SE-35, E.R. Engdahl, ed.: pp. 36–40. Boulder: World Data Center (A) for Solid Earth Geophysics 1984

Červený, V., Ravindra, R.: Theory of seismic head waves. Toronto: University of Toronto Press 1971

Červený, V., Molotkov, I.A., Pšenčík, I.: Ray method in seismology. Praha: Karlova Universita 1977

Dravinski, M.: Scattering of plane harmonic *SH* wave by dipping layers of arbitrary shape. Bull. Seismol. Soc. Am. **73**, 1303–1319, 1983

Futterman, W.I.: Dispersive body waves. J. Geophys. Res. **67**, 5279–5291, 1962

Hong, T.L., Helmberger, D.V.: Glorified optics and wave propagation in nonplanar structure. Bull. Seismol. Soc. Am. **68**, 1313–1330, 1978

Johnson, L.R., Silva, W.: The effects of unconsolidated sediments upon the ground motion during local earthquakes. Bull. Seismol. Soc. Am. **71**, 127–142, 1981

Kjartansson, E.: Constant Q wave propagation and attentuation. J. Geophys. Res. **84**, 4737–4748, 1979

Klem-Musatov, K.D., Aizenberg, A.M.: The ray method and the theory of edge waves. Geophys. J.R. Astron, Soc. **79**, 35–50, 1984

Kohketsu, K.: 2-*D* reflectivity method and synthetic seismograms for irregularly layered structures – I. *SH*-wave generation. Geophys. J.R. Astron. Soc. **89**, 821–838, 1987

Kravtsov, Yu.A., Orlov, Yu.I.: Geometrical optics of inhomogeneous media (in Russian). Moscow: Nauka 1980

Krebes, E.S.: The viscoelastic reflection/transmission problem: two special cases. Bull. Seismol. Soc. Am. **73**, 1673–1683, 1983

Langston, Ch.A., Lee, J.J.: Effect of structure geometry on strong ground motions: the Duwamish river valley, Seattle, Washington. Bull. Seismol. Soc. Am. **73**, 1851–1863, 1983

Lee, J.J., Langston, Ch.A.: Three-dimensional ray tracing and the method of principal curvature for geometric spreading. Bull. Seismol. Soc. Am. **73**, 765–780, 1983a

Lee, J.J., Langston, Ch.A.: Wave propagation in a three-dimensional circular basin. Bull. Seismol. Soc. Am. **73**, 1637–1653, 1983b

Moczo, P., Červený, V., Pšenčík, I.: Documentation of earthquake algorithm – RESPO (program package). In: Short description of computer programs for studying seismic response of near-surface geological structures, J. Zahradník, ed.: pp. 14–17. Prague: Inst. Geophysics, Charles University 1985

Moczo, P., Červený, V., Pšenčík, I.: Application of ray method in seismic response analysis. In: Proc. of the 3rd Inter. Symp. on the Analysis of Seismicity and on Seismic Risk, V. Schenk, Z. Schenková, eds., vol. II, pp. 455–463. Prague: Geophys. Inst. Czechosl. Acad. Sci. 1986

Mueller, G.: Rheological properties and velocity dispersion of a medium with power-law dependence of Q on frequency. J. Geophys. **54**, 20–29, 1983

Nowack, R., Aki, K.: The two-dimensional Gaussian beam synthetic method: testing and application. J. Geophys. Res. **89**, 7797–7819, 1984

Sanchez-Sesma, F.J., Bravo, M.A., Herrera, I.: Surface motion of topographical irregularities for incident *P*, *SV* and Rayleigh waves. Bull. Seismol. Soc. Am. **75**, 263–269, 1985

Virieux, J.: *SH*-wave propagation in heterogeneous media: velocity-stress finite-difference method. Geophysics **49**, 1933–1957, 1984

Yerokhin, L.Yu.: The seismic propagation in a valley with semi-elliptical boundary (in Russian). Izv. Akad. Nauk SSSR, Fizika Zemli, No. 8, 60–73, 1985

Zahradník, J., Hron, F.: Seismic ground motion of sedimentary valley La Molina, Lima, Peru. In: Proc. of the 3rd Inter. Symp. on the Analysis of Seismicity and on Seismic Risk, V. Schenk, Z. Schenková, eds., vol. II, pp. 340–346. Prague: Geophys. Inst. Czechosl. Acad. Sci. 1986

Zahradník, J., Urban, L.: Effect of a simple mountain range on underground seismic motion. Geophys. J.R. Astron. Soc. **79**, 167–183, 1984

Received May 18, 1987; revised version August 14, 1987
Accepted August 17, 1987